Estimation of Blood Pressure from Arterial Blood Pressure using PPG Signals

Teodora Mladenovska, Ana Madevska Bogdanova, Magdalena Kostoska, Bojana Koteska, Nevena Ackovska
Ss. Cyril and Methodius University,
Faculty of Computer Science and Engineering
Skopje, North Macedonia
mladenovska.teodora@students.finki.ukim.mk,
{ana.madevska.bogdanova, magdalena.kostoska, bojana.koteska,
nevena.ackovska }@finki.ukim.mk

***Abstract*—Predicting Blood pressure from Photoplethysmography (PPG) signals is an active area of research and there have been many studies exploring the feasibility of this approach.**

This paper elaborates a technique for estimaton of continuous Arterial blood pressure (ABP) waveform using PPG signals as inputs in a developed deep learning model. The ultimate goal is estimating the Blood pressure, but unlike the standard regression models for predicting the Blood pressure by systolic BP (SBP) and Diastolic BP (DBP), this approach calculates SBP and DBP from the estimated ABP waveform, which enable further analysis to enhance the BP estimation. The best obtained results are MAE of 8.40mmHg, and a MAE of 11.1mmHg and 7mmHg for SBP and DBP respectively. The promising prediction of SBP and DBP using our proposed machine learning model has the potential to improve clinical decision-making and resource allocation process in emergency situations.

***Keywords*—blood pressure (BP) estimation, electrocardiogram (ECG), photoplethysmography (PPG), gated recurrent unit (GRU), artificial neural network, deep learning**

I. Introduction

Blood pressure (BP) is an important vital sign that can provide valuable information about a person's health status. Blood pressure is the force exerted by the blood against the walls of blood vessels, and it is an essential measure of cardiovascular health. It is measured using two numbers: systolic pressure, which measures the force of blood when the heart beats, and diastolic pressure, which measures the force of blood when the heart is at rest.A healthy blood pressure reading is typically around 120/80 mmHg, with the systolic BP being at the top and the diastolic BP being at the bottom. High blood pressure, or hypertension, can increase the risk of heart disease, stroke, and other health complications, while low blood pressure can cause dizziness, fainting, and other symptoms [1]. Traditional methods for measuring blood pressure typically involve using a cuff to measure the pressure in the brachial artery. However, non-invasive methods for estimating blood pressure have been gaining popularity in recent years. One promising approach for estimating blood pressure non-invasively is through the analysis of photoplethysmography (PPG) signals. PPG signals are generated by measuring changes in the blood volume in peripheral blood vessels, such as those in the fingertip. PPG signals are collected from pulse oximeters that produce visible light (LED) on the skin and measure the micro-variations in the transmitted or reflected light intensity through a photodiode [2]. If we have an ABP signal, by calculating the maximum and minimum values in the ABP segment, we can obtain the SBP and DBP, respectively. In recent years, advances in machine learning and signal processing techniques have enabled researchers to develop algorithms for estimating SBP and DBP from PPG signals. These algorithms typically involve analyzing the PPG waveform and extracting features that are correlated with the BP. Machine learning models can then be trained on these features to predict the BP from PPG signals [3], [4]. In our study, we are building a model that estimates an ABP waveform from PPG signals.

II. Related Work

There are several published papers where the ABP waveform is estimated. In [5], which is known as PPG2ABP, they used two deep learning models to estimate the ABP waveform. An approximation network, which is a one-dimensional U-Net network with an input of a PPG signal, was first used to approximate the waveform. They then used a refinement network to fix the estimated ABP waveforms. A 1D MultiResUNet model was used to improve the model. According to another study [6], calculating ABP waveforms might be done solely with a 1D-modified U-Net network. A different preprocessing technique was employed in another work [7], which predicts the ABP waveform using U-Net. LeNet-5 and U-Net, two deep convolution autoencoders used to predict the ABP waveforms, are compared in [8]. Using the cross-validation (CV) method, data generalization was investigated. The outcomes show that the U-Net works better than alternative estimating techniques for SBP values. The LeNet-5, however, is slightly better to predict DBP values. The ensemble of CV models is then optimized using a deep convolutional autoencoder (GDCAE) based on a genetic algorithm. The results show that the GDCAE performs better than the LeNet-5 and the U-Net. Consequently, the review discusses the results of the model GDCAE that performed the best. Unfortunately, combining two deep learning algorithms to get two distinct values requires a lot of parameters, which is computationally inefficient. The combination of two separate models can obtain two values, and no optimal model for predicting the resulting ABP waveform

was generated as an outcome. In [9], a 1D V-Net deep learning system for ABP waveform prediction was proposed. Two signals (ECG and PPG), with a 4s window, were used as input to the model, along with several constant values. At each timestamp, constants were encoded and treated as extra channels. The following constants were used: the most recent noninvasive SBP, DBP, and MAP values obtained prior to the window, the time interval between these measurements, the standard deviation (STD) and median of the pulse arrival time, and the pulse rate. The PPG and ABP waveforms at the input differ from one another. The residual error can be learned by the model thanks to the manner it was built. Another recent paper [10], suggested using PPG data as input to a cycle generative adversarial network (CycleGAN) to predict ABP waveforms. Despite the fact that the bulk of the publications used an encoder-decoder technology, they employed an innovative technique to estimate the waveforms by using a generator and a discriminator network.

III. Materials and Methods

In this section, we describe the dataset, the developed technique for data preprocessing part and the model, as well as the used evaluation metrics.

A. Dataset

The MIMIC-III (Medical Information Mart for Intensive Care III) dataset is a freely available collection of de-identified health-related data. It contains data from over 40,000 patients who were admitted to the intensive care units (ICUs) of a large tertiary care hospital between 2001 and 2012 [11]. We do not use the entire MIMIC-III dataset in our research, but rather a subset of it. The dataset we work with consists of 508 signals, sampled at Fs = 125 samples/sec for 126 patients. In the dataset, we are only considering the files where the PPG and ABP signals are represented in the entire window, without null values and the window size is in the range between 1.4 and 80s. For the preparation of the input vectors for the problem at hand, besides setting the PPG signal, we are introducing the first and second PPG signal derivatives [3], and the model's output is a raw ABP signal.

B. Preprocessing

One of the main problems obstructing full exploitation of the available biomedical databases resides in archiving these data without any concern about their quality. Thus, before we start training the models, we need to preprocess the data by implementing some preprocessing techniques that are used when working with biomedical signals and time series data. The process of data preprocessing takes place in the following stages: filtering and normalization, segmentation and correlation. Also, we introduced the alignment technique (between PPG and APB) since the model's output is an ABP waveform.

1) Filtering and normalization: The construction of PPG sensors makes them susceptible to motion artifacts (MA), which lead to signal quality distortion. The most significant causes of MA include changes in blood flow caused light seeping through the space between the sensor and the skin and physical activity, which may affect where the sensor is placed on the skin [12]. The data filtering process starts by filtering the PPG signals, using the Python Neurokit toolbox with a sampling rate of 125Hz. Scaling is done by using the MinMaxScaler after the data has been cleaned. It consists of two separate scalers, one for scaling the input signal's values and the other for scaling the output signal's values. After this step, the signals are positioned at the same range of values, allowing signal alignment and determining whether they are correlated.

2) Signal alignment: During the development of the model for the ABP estimation, it was acknowledged that ABP and PPG signals need an alignment when creating the input (PPG) and the output (ABP) for the dataset. ABP and PPG measurements are frequently provided without time alignment (out of phase), since they are typically made using various techniques and taken from different areas of the body (e.g., arm vs. wrist) [13]. A few methods for fixing the phase difference have recently been published [14], [15], [16], [17]. The alignment has been carried out for all records using cross-correlation. The cross-correlation function is defined as:

$$g(\Delta t) = \sum \mathrm{ABP}(t) \times \mathrm{PPG}(t + \Delta t)$$

Fig. 1 shows a histogram with the phase difference of the used signals. This phase difference is determined by the cross-correlation of the ABP and PPG signals, then the location of the maximum value has been considered as time lead or lag. The signals are aligned after determining the lag between them, since they are obtained from the same source.

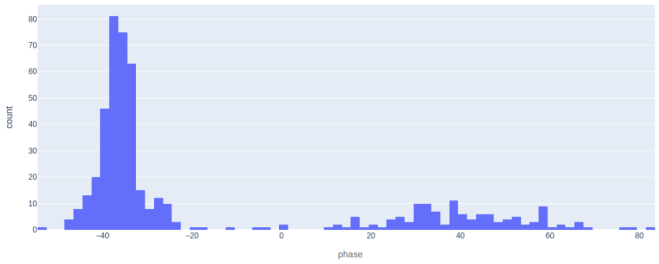

Fig. 1. Phase difference between ABP and PPG

3) Segmentation and correlation: Segmentation is performed by dividing the signals into smaller chunks with a window size of 1.4s. From the results of the undertaken analyses, it can be concluded that there is a similarity between the PPG and ABP morphologies. This is reflected in the correlation coefficient calculated after the alignment. Pearson's

correlation coefficient is used to determine how similar PPG and ABP are in terms of morphology. The value of r ranges from -1 to +1, where the value close to +1 or -1 means that signals have strong positive or negative similarity, respectively; otherwise, the value is close to zero [18]. The correlation coefficient is calculated as follows:

$$r = \frac{n\sum XY - \sum X \sum Y}{\sqrt{n\sum X^2 - (\sum X)^2} - \sqrt{n\sum Y^2 - (\sum Y)^2}}.$$

As suggested in the literature, the PPG and the ABP signals are morphologically correlated if the correlation factor r>0.9 [18]. Hence, we rejected the signals with a correlation lower than 0.9. Additionally, the ABP signals' maximum and minimum values are calculated; if the minimum value is lower than 40 (DBP < 40) or the maximum value is higher than 220 (SBP > 220), the signal is considered out of our working scope and consequently - denied.

After the entire process of preprocessing and segmentation, a dataset of 5113 PPG and ABP signals is obtained. From the total number of data, 4641 are assigned to the training set, 105 to the testing set, and 367 to the validation set. The division of the sets is done before the segmentation process, which means that the patients from the training set do not appear in the testing and the validation set, and vice versa - the patients from the testing set do not appear in the training and the validation set. The set partitioning is done according to the ratio of 85% of patients for training, 7% of patients for validation, and 8% of patients for testing, where all of the patients have a different number of records and the length of each record could differ.

C. Model Structure

In this paper, we are using a deep neural network model, the Gated Recurrent Unit (GRU). GRU is a type of Recurrent Neural Network (RNN) that, in certain cases has advantages over long short term memory networks (LSTM). GRU uses less memory and is faster than LSTM [19].

The network we have built consists of one GRU input layer with 522 neurons, and three GRU hidden layers of 350, 240, and 182 neurons each followed by a ReLU activation function. After the second hidden layer, there is a Dropout layer with a value of 0.1. The last hidden layer is flattened and on the output, there is a Dense layer with 175 neurons. The model was trained on 100 epochs on a batch size of 32, using Adam optimizer with a learning rate of 0.0001 and checkpoints for early stopping and saving the best model.

D. Evaluation Metrics

The evaluation process is done by the following evaluation metrics: MAE and MSE [20]. Mean Squared Error (MSE) - L2 loss function and Mean Absolute Error (MAE) - L1 loss function are the most prevalently used loss function for regression. For predicted values $\hat{Y} = \{\hat{y}1 , \hat{y}2 , \hat{y}3, \ldots , \hat{y}n\}$ and the target values $Y = \{y1 , y2 , y3 , \ldots , yn\}$, they are defined as follows:

$$MSE = \frac{\sum_{i=1}^{n}(y_i - \hat{y}_i)^2}{n}$$

$$MAE = \frac{\sum_{i=1}^{n}|y_i - \hat{y}_i|}{n}$$

In our experiments, we are using MSE as a loss function of the network - the penalty is not proportional to the error but to the square of the error. Squaring the error gives higher weight to the outliers, which results in a smooth gradient for small errors.

IV. Results and Discussion

After training the model, it is evaluated on the prepared test data, with the following outcomes.

Metrics	SBP	DBP
MSE	195	75
MAE	11.1	7

TABLE I
EVALUATION METRICS

Table I shows that the obtained results regarding MAE are promising, although MAE can fail to punish large errors in prediction. This analysis is somewhat confirmed since there are significant differences between MAE and MSE values.

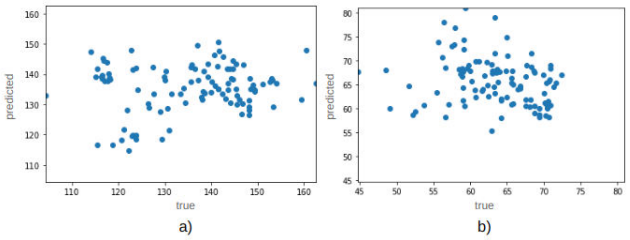

Fig. 2. True and predicted values: a) SBP, b)DBP

Figure 2 presents the actual and predicted values of SBP (a) and DBP (b) for each test data point. These visualizations can help in model improvement in a way that one can analyse each data point separately, and address directly the ones above some acceptable error threshold. Figure 2 also shows that there isn't a single person in the testing dataset with a DBP of 80 (which is considered normal blood pressure) or above, while it is not the case for the whole dataset. To overcome this issue, in the future, we could use the cross-validation technique, for better utilization of our data. There is one additional results representation that shows us percentages of the data that have errors according to different thresholds (Table II).

	<3	<5	<10	<15	>15
SBP	19%	30.5%	53.3%	67.6%	32.4%
DBP	28.6%	41.9%	78.1%	90.5%	9.5%

TABLE II
CUMULATIVE ERROR IN PERCENTAGE

The following Fig. 3 presents the differences between the actual and the estimated ABP waves for two different model inputs. The blue line represents the true values and the orange represents the predicted ones. It is evident that the forms are very similar, though the max (SBP) and min (DBP) values are not very close. Nevertheless, the morphological analysis of the ABP signal can help in producing different features for building a better dataset.

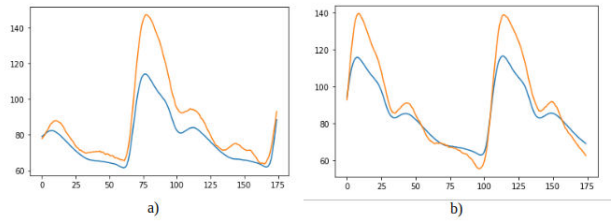

Fig. 3. True and predicted ABP waveform, a) entry 1 and b) entry 2

V. Conclusion

In this research, through our suggested model, we attempted to estimate Arterial Blood Pressure (ABP) waveforms from Photoplethysmogram (PPG) signals. With this approach, we can estimate the ABP waveform, which can be used to estimate cardiovascular anomalies from the waveform patterns of the PPG signal, in contrast to studies that only attempted to predict discrete BP parameters, such as SBP, DBP, MAP. ABP waveforms, which are generally collected invasively, can now be estimated from externally acquired PPG signals. Contrary to some studies, which used ECG signals alongside PPG to estimate ABP, we decided to process only the PPG signals, whilst reaching promising performance in the estimation process. As a future work, we will focus on improving model performances, trying different networks and models, as well as enriching the dataset with new data.

Acknowledgment

This paper has been written thanks to the support of the "Smart Patch for Life Support Systems" - NATO project G5825 SP4LIFE and by the National project IBS4LIFE of Faculty of Computer Science and Engineering, at Ss. Cyril and Methodius University in Skopje.

References

[1] "Blood pressure symptoms," [retrieved: Mar, 2023]. [Online]. Available: https://www.diabetes.co.uk/high-low-blood-pressure-symptoms.html

[2] Susha Cheriyedath, "Photoplethysmography (ppg)," [retrieved: Mar, 2023]. [Online]. Available: https://www.news-medical.net/health/Photoplethysmography-(PPG).aspx

[3] L. Y. Harfiya LN, Chang CC, "Continuous blood pressure estimation using exclusively photopletysmography by lstm-based signal-to-signal translation," National Library of Medicine, National Center for Biotechnology Information, 04 2021.

[4] A. Tazarv and M. Levorato, "A deep learning approach to predict blood pressure from ppg signals," CoRR, vol. abs/2108.00099, 05 2021.

[5] N. Ibtehaz, S. Mahmud, M. E. H. Chowdhury, A. Khandakar, M. A. Ayari, A. Tahir, and M. S. Rahman, "Ppg2abp: Translating photoplethysmogram (ppg) signals to arterial blood pressure (abp) waveforms using fully convolutional neural networks," 2022.

[6] T. Athaya and S. Choi, "An estimation method of continuous non-invasive arterial blood pressure waveform using photoplethysmography: A u-net architecture-based approach," Sensors, vol. 21, no. 5, 2021. [Online]. Available: https://www.mdpi.com/1424-8220/21/5/1867

[7] R. V. K, V. S, P. G, A. K, N. K. M, and V. Vijayaraghavan, "Bp-net: Efficient deep learning for continuous arterial blood pressure estimation using photoplethysmogram," 2021.

[8] M. Sadrawi, Y.-T. Lin, C.-H. Lin, B. Mathunjwa, S.-Z. Fan, M. F. Abbod, and J.-S. Shieh, "Genetic deep convolutional autoencoder applied for generative continuous arterial blood pressure via photoplethysmography," Sensors, vol. 20, no. 14, 2020. [Online]. Available: https://www.mdpi.com/1424-8220/20/14/3829

[9] B. L. Hill, N. Rakocz, Á. Rudas, J. N. Chiang, S. Wang, I. Hofer, M. Cannesson, and E. Halperin, "Imputation of the continuous arterial line blood pressure waveform from non-invasive measurements using deep learning," Scientific reports, vol. 11, no. 1, p. 15755, 2021.

[10] M. A. Mehrabadi, S. A. H. Aqajari, A. H. A. Zargari, N. Dutt, and A. M. Rahmani, "Novel blood pressure waveform reconstruction from photoplethysmography using cycle generative adversarial networks," in 2022 44th Annual International Conference of the IEEE Engineering in Medicine & Biology Society (EMBC). IEEE, 2022, pp. 1906–1909.

[11] A. E. Johnson, T. J. Pollard, L. Shen, L. wei H. Lehman, M. Feng, M. Ghassemi, B. Moody, P. Szolovits, L. A. Celi, and R. G. Mark, "Mimic-iii, a freely accessible critical care database," National Library of Medicine, National Center for Biotechnology Information, 05 2016.

[12] M. Elgendi, "On the analysis of fingertip photoplethysmogram signals," Current cardiology reviews, vol. 8, pp. 14–25, 02 2012.

[13] A. F., D. P. L, D. N. A., S. M., and L. AML., "Photoplethysmography signal wavelet enhancement and novel features selection for non-invasive cuff-less blood pressure monitoring." National Library of Medicine, National Center for Biotechnology Information, 02 2023.

[14] S. M. Xing X, "Optical blood pressure estimation with photoplethysmography and fft-based neural networks." National Library of Medicine, National Center for Biotechnology Information, 07 2016.

[15] L. N. Harfiya, C.-C. Chang, and Y.-H. Li, "Continuous blood pressure estimation using exclusively photopletysmography by lstm-based signal-to-signal translation," Sensors, vol. 21, no. 9, p. 2952, 2021.

[16] X. Xing and M. Sun, "Optical blood pressure estimation with photoplethysmography and fft-based neural networks," Biomedical optics express, vol. 7, no. 8, pp. 3007–3020, 2016.

[17] H. Shin and S. D. Min, "Feasibility study for the non-invasive blood pressure estimation based on ppg morphology: Normotensive subject study," Biomedical engineering online, vol. 16, pp. 1–14, 2017.

[18] G. M. Aguilar, N. Howard, D. Abbott, K. Lim, R. Ward, and M. Elgendi, "Can photoplethysmography replace arterial blood pressure in the assessment of blood pressure?" Journal of Clinical Medicine, vol. 7, p. 316, 09 2018.

[19] S. Saxena, "Introduction to gated recurrent unit (gru)," [retrieved: Mar, 2023]. [Online]. Available: https://www.analyticsvidhya.com/blog/2021/03/introduction-to-gated-recurrent-unit-gru/

[20] J. Brownlee, "Regression metrics for machine learning," [retrieved: Mar, 2023]. [Online]. Available: https://machinelearningmastery.com/regression-metrics-for-machine-learning/